

Structural and vibrational properties of amorphous phosphorus

B. V. Shanabrook* and J. S. Lannin

Department of Physics, The Pennsylvania State University, University Park, Pennsylvania 16802

(Received 17 February 1981)

Thin films of amorphous P, prepared by rf sputter deposition under conditions of variable substrate temperature, have been studied using x-ray diffraction and Raman scattering methods. The low-angle x-ray spectra indicate a peak at $k \simeq 1.1 \text{ \AA}^{-1}$, whose half-width and relative intensity are a continuous function of deposition temperature. The diffraction spectra provide evidence for continuously variable intermediate-range order as a function of deposition temperature. The polarized and depolarized Raman components indicate substantial changes with deposition temperature associated with the development of a number of high-frequency spectral features. Modifications of the depolarized Raman spectra, as well as differences between the phonon density of states and depolarized bulk spectra, provide additional evidence for intermediate-range order. The x-ray and Raman spectra imply structural and dynamical correlations in amorphous solids of intermediate range and further suggest that such correlations are continuously variable. The experimental results are discussed in terms of a layerlike model with variable intralayer and interlayer correlations. As in crystalline solids, it appears that structural correlations are a prerequisite for dynamical correlations for optical-like modes.

INTRODUCTION

In crystalline solids the presence of periodicity, which leads to Bloch's theorem, results in physical properties that are appreciably influenced by spatial and temporal correlations. Thus long-range order in finite temperature or dilute impurity lattices results in spatial and temporal correlations of the wave functions for electrons as well as phonons. In contrast to crystalline solids, it has often been assumed that amorphous solids have limited spatial correlations, so that temporal correlations beyond those associated with short-range order are not significant. It is, however, of interest to inquire if nonperiodic solids may be prepared in a state of intermediate-range order and whether, by analogy with periodic systems, correlation effects will occur in the phonon and electron wave functions over this range. A related important point is the question of whether structural and dynamical correlations in nonperiodic solids may be continuously variable.

Information about intermediate-range order and the question of correlations in phonon and electron states may in principle be obtained by elastic as well as inelastic scattering experiments. In a number of elemental amorphous semiconductors, as well as in bulk binary chalcogenide glasses and liquids,^{1,2} x-ray-diffraction measurements yield a

peak at low scattering vectors, $\sim 1 \text{ \AA}^{-1}$. While the general structural conditions for the observation of this "anomalous" peak are unclear, it is generally believed^{1,3} that it is a manifestation of structural correlations over an intermediate range. In contrast to diffraction studies, Raman scattering measurements may provide information about dynamical correlations that arise from phonon induced fluctuations in electronic polarizability. Intuitively, the existence of intermediate-range order is expected to modify the phase relation of atomic displacements and thus the Raman scattering spectra relative to that of a system with only short-range order.

In thin-film and bulk amorphous (*a-*) As it has been suggested that large variations in the Raman spectra and specific heat arise from changes in intermediate-range order.^{4,5} Neutron scattering studies⁶ also suggest coherency effects in *a-*As associated with intermediate-range order. Selected vibrational modes in the bulk binary chalcogenide^{3,7} and oxide⁸ glasses have also been interpreted as manifesting order beyond short range. The evidence to date for intermediate-range order based on vibrational probes has not, however, been conclusive. A recent theoretical study⁹ has considered the role of structural correlations on the Raman scattering response for the polarized and depolarized spectral components. This work has indicated

that the depolarized component will tend to manifest the general form of the phonon density of states unless intermediate-range order is present. If such order exists, however, then it is possible that certain vibrational states may yield dynamical correlations that result in a depolarized spectrum modified from that of the phonon density of states. This theory was applied to a binary AX_2 tetrahedral glass of GeO_2 , for which it was determined that intermediate-range order was absent. It is therefore useful to determine if other amorphous solids may indicate the presence of intermediate-range order based on the above criterion. In contrast to binary systems, elemental amorphous materials allow for an improved test of this theory as a reasonable estimate of the phonon density of states may be obtained, unencumbered by differences in neutron cross sections.

In the present study, complementary x-ray diffraction and Raman scattering measurements have been performed on thin-film elemental *a*-P prepared by rf sputtering. In bulk form, *a*-P indicates the aforementioned low-angle diffraction peak^{10,11} as well as considerable detail in the Raman¹¹ and infrared-absorption¹² spectra that are suggestive of intermediate-range order. The results presented below represent the first systematic comparison of the structural and vibrational properties of an amorphous solid which allow information to be obtained about correlation effects and their variability. The experimental results in *a*-P indicate that, as in periodic systems, structural correlations are a general necessary condition for dynamical correlations, for high-frequency, optical-like modes.

EXPERIMENT

A commercial Material Research Corporation sputtering system was employed for thin-film preparation. Thin films of *a*-P of $\sim 20\text{-}\mu\text{m}$ thickness were prepared by rf sputtering at an argon pressure of $60\ \mu\text{m}$ and a power of 100 W. The target-to-substrate distance was $\sim 5\ \text{cm}$. Since the sputtering parameters of pressure, power, substrate distance, and geometry all affect the energy distribution of the incoming sputtered species and resultant film properties, it is necessary to carefully control the sputtering parameters. The properties of the films were varied by independently changing only the substrate temperature via a heater. Accurate surface temperature measurements were attained with Ag-Al thin-film thermocouples¹³ deposited on polished Si wafers. The rather large

sputtering gas pressure results in a mean free path of sputtered atoms of $\sim 0.2\ \text{cm}$. Stirling and Westwood¹⁴ estimated that thermal equilibrium between the sputtered atoms and the sputtering gas occurs after ~ 10 collisions. As the target-to-substrate distance is ~ 25 mean free paths, the sputtered atoms are essentially thermalized when condensed on the substrate. Under these conditions, the substrate temperature should be an important parameter in the film formation process. Raman scattering, infrared absorption, and x-ray diffraction measurements were performed on thin *a*-P films prepared at substrate temperatures between $0\text{--}177^\circ\text{C}$. The large vapor pressure of P films at temperatures greater than 200°C limited the preparation of higher temperature films, while the rf sputtering system design prevented films from being formed below 0°C .

The film thermocouples were used to directly monitor the surface temperature of the substrate immediately *after* deposition, as differences in potential in the sputtering chamber due to rf induction effects result in inaccurate temperature measurements during deposition. However, the use of a calibrated thin film amorphous Ge resistance probe¹⁵ indicated temperature readings during sputtering which were negligibly different from those immediately after sputtering.

RESULTS

In Fig. 1 the x-ray diffraction spectra of selected rf sputtered films are shown for substrate temperatures T_s of 0, 94, and 177°C . The spectra are similar in form for scattering vectors $k = 4\pi \sin\theta/\lambda$ greater than $1.5\ \text{\AA}^{-1}$ and have thus been normalized to the intensity I_2 shown. As the peak at $2.3\ \text{\AA}^{-1}$ as well as higher peaks are primarily determined by the nearest-neighbor distance, this normalization procedure is a useful first approximation for determining the relative intensity of the low-angle peak I_1 . Additional contributions to the scattering which determine the actual intensity above background are assumed to be relatively constant. A more detailed determination of changes in the scattering function¹⁶ $F(k)$ with T_s are, however, prohibitively difficult for *a*-P given its small x-ray absorption cross section and the requirement for rather thick films.

With increasing substrate temperature, Fig. 1 qualitatively indicates a rise in the ratio I_1/I_2 as well as a narrowing of the lowest diffraction peak at $1.08\ \text{\AA}^{-1}$. The latter peak is, however, observed

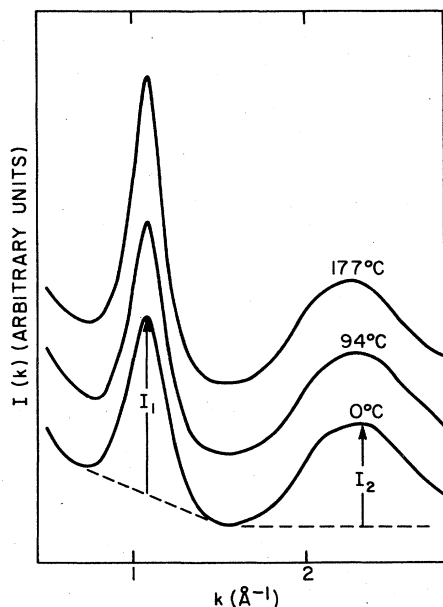


FIG. 1. Selected x-ray diffraction spectra of rf sputtered *a*-P films for the substrate temperatures shown.

to occur at the same k value for films deposited under conditions of fixed sputtering geometry, pressure, and cathode voltage. The position of this peak occurs somewhat above the $k = 1.04 \text{ \AA}^{-1}$ value of bulk *a*-P prepared by polymerization of liquid P. Figure 2 indicates in a more quantitative manner the substrate temperature variation of I_1/I_2 as well as the inverse width of the low-angle peak; the width corresponds to the full width at half maximum. As Fig. 2 indicates, the inverse width of the low-angle peak is observed to vary essentially linearly with T_s . In contrast, the intensity ratio I_1/I_2 indicates a weak variation at low T_s with a more rapid increase ensuing at $T_s \approx 75^\circ\text{C}$. At high T_s this ratio appears to saturate to a value of $I_1/I_2 \approx 2.8$. The position of the low scattering vector peak k_1 has been indicated as an inverse measure of a quasiperiodic structural repeat distance.¹ Fourier inversion suggests that this distance is of order $2\pi/k_1$. For the data of Fig. 2 this yields $2\pi/k_1 = 5.8 \text{ \AA}$. The inverse half-width of the low- k peak has similarly been attributed to an associated structural correlation length, l_s . One rough estimation procedure for l_s uses the Debye-Scherrer equation derived for small crystallites of mean dimension $\bar{D} = 2\pi c / \Delta k$, where Δk is the peak width in \AA^{-1} and c is a numerical factor between 0.9–1.4.¹⁶ If l_s is equated to \bar{D} , then for $c = 0.9$, $l_s = 29 \text{ \AA}$ for the highest temperature film.

In contrast, for the 0°C film this value decreases by 30%. Though no theoretical justification has been given for extending the Debye-Scherrer equation to amorphous solids, it is reasonable to expect that it yields, within most likely a factor of ~ 2 , an estimate of the structural correlation length. Independent of the precise values of l_s it is reasonable to assume that the inverse half-width variation of 30% for the films studied in Fig. 2 is a *quantitative* measure of the relative change in structural correlation length with T_s . For a layerlike model, discussed below, l_s may be associated with an inter-layerlike correlation length.¹

Figure 2 indicates that I_1/I_2 has a different variation than the inverse width and as such is a second measure of structural order. In crystalline solids the effect of "phonon disorder," associated with finite temperatures, is to reduce diffraction peak intensities by the Debye-Waller factor, while preserving the width of the peaks. The ratio I_1/I_2 is thus an alternative means of viewing the role of disorder in amorphous solids and has a somewhat more intuitive justification than the area, e.g., of the lowest peak. While no detailed theoretical interpretation has been presented for this ratio, Bishop and Shevchik¹⁷ have suggested that for a layerlike model it is a relative measure of the "fraction of material in the layer structure." For the films of Fig. 2, I_1/I_2 is found to increase by 55% between the lowest and highest T_s values. In contrast to the peak position and a half-width in bulk

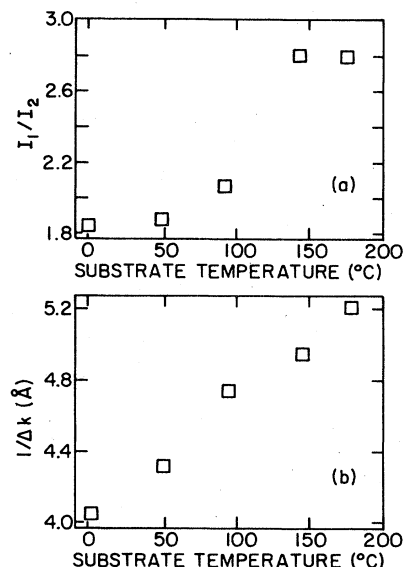


FIG. 2. Variation of the x-ray diffraction intensity ratio, I_1/I_2 (a) and low-angle peak width, $1/\Delta k$ (b) as a function of substrate temperature.

a-P, which are similar to that of the highest T_s film, this is not the case for I_1/I_2 . In bulk *a*-P this ratio is 2.3, or $\sim 20\%$ lower than the value for the highest T_s film.

The HH Raman scattering spectra of the rf sputtered films prepared between 0–177°C are shown in Fig. 3. These spectra exhibit rather striking differences as a function of increasing T_s for amorphous solids. This is noted both in the evolution of peaks in the range between 200–300 cm^{-1} and at higher frequencies. In addition, various spectral minima are enhanced at higher T_s values. Specifically, the features indicated by the arrows in Fig. 3 at 210, 280, 350, 380, and 500 cm^{-1} of the HH spectra become more prominent in the higher T_s films. The minima or pseudogaps at $\sim 165 \text{ cm}^{-1}$ also become deeper for the higher T_s films. A comparison of these sputtered results with those of bulk *a*-red-P, also shown in Fig. 3, indicates a number of similarities. This is particularly the case for the film prepared at 177°C. Although the bulk and 177°C film spectra are similar, some

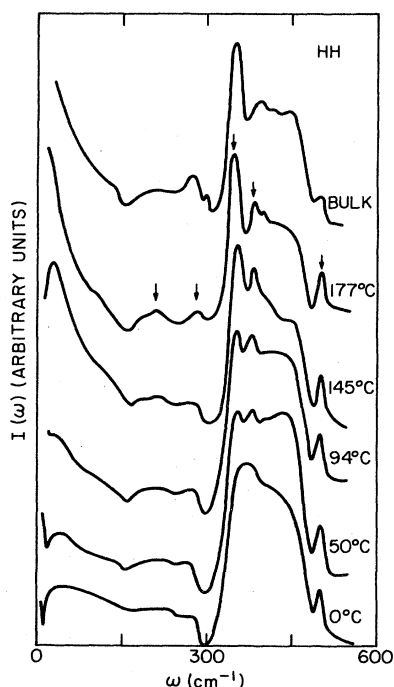


FIG. 3. A comparison of the 80-K HH Raman spectra of rf sputtered *a*-P films prepared at the indicated T_s . The arrows indicate features exhibiting large changes. The Raman spectrum of bulk *a*-red-P is also shown. The HH designation corresponds to incident and scattering fields within the scattering plane.

differences are noted in the relative intensities of features at 210, 280, 300, 380, and 500 cm^{-1} . A very weak feature occurs at $\sim 300 \text{ cm}^{-1}$ in the sputtered data, in contrast to a stronger feature in the bulk *a*-P. This weak peak, which is not visible on Fig. 3, is $\sim \frac{1}{30}$ the intensity of the 500 cm^{-1} feature. This intensity ratio is rather constant for all of the HH Raman spectra of the rf sputtered films, in which the 300 cm^{-1} peak could be observed within signal-to-noise ratio.

Shown in Fig. 4 is an analysis of the T_s dependence of the relative intensity of the major feature observed at 350 cm^{-1} . As the measurement of the absolute intensity is sensitive to the absorption coefficient, which is itself a function of T_s ,¹⁸ and alignment of the sample, the ratio of the intensities at 350 and 440 cm^{-1} , $R_{\text{HH}}(350)$, is shown in Fig. 4. This ratio appears to be a reasonable normalization procedure, as the intensity variation at $\sim 440 \text{ cm}^{-1}$ is relatively weak and exhibits the least amount of relative change in shape for the higher optical band as a function of T_s . As Fig. 4 indicates, this ratio increases by $\sim 90\%$ between T_s values of 0 and 177°C, and indicates the increasing prominence of the peak at 350 cm^{-1} . The intensities of features occurring at ~ 380 and 500 cm^{-1} are observed to exhibit similar behavior with increasing T_s , as they vary proportional to the peak at 350 cm^{-1} .

The sharp Raman features in bulk *a*-As at 165 and 280 cm^{-1} which correspond to those at 300 and 500 cm^{-1} have been attributed to bonding coordination defects.^{19,20} We have observed that the Raman scattering features in *a*-P films become larger with increasing T_s . Furthermore, the Raman intensities at 300, 350, 380, and 500 cm^{-1} appear interrelated. As the concentration of bonding

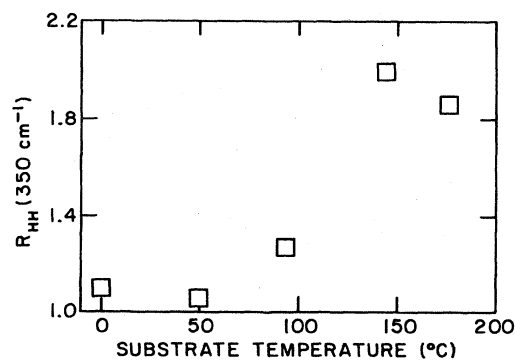


FIG. 4. The T_s behavior of the Raman ratio, $R_{\text{HH}}(350 \text{ cm}^{-1})$, where $R_{\text{HH}}(350 \text{ cm}^{-1}) = I_{\text{HH}}(350 \text{ cm}^{-1})/I_{\text{HH}}(440 \text{ cm}^{-1})$.

coordination defects might be expected to become smaller for the higher T_s films and since the Raman intensity of features at 300 and 500 cm^{-1} appear related to features of a normally coordinated a -P network, we suggest that the defect model requires modification.

The depolarized VH Raman scattering spectra of the rf sputtered films are shown in Fig. 5. As in the HH results, distinct features at 160, 210, 280, 350, 380, and 500 cm^{-1} become more well defined in the higher T_s films. The lowest-frequency peak, below 50 cm^{-1} is also observed to decrease in frequency as T_s is increased. This peak is observed to occur at $\sim 12 \text{ cm}^{-1}$ and $\sim 42 \text{ cm}^{-1}$ for films prepared at 177 and 0°C, respectively. Although the larger background contribution in the 177°C film could result in the appearance of a shifting of the low-frequency peak, the largest possible shift is $\sim 12 \text{ cm}^{-1}$. This implies that the low-frequency peak of the film prepared at 177°C occurs at least 18 cm^{-1} below the corresponding peak in the 0°C film. If the low-frequency peak Raman coupling parameters are not significantly different for these films, the spectra imply a shift of the low-frequency

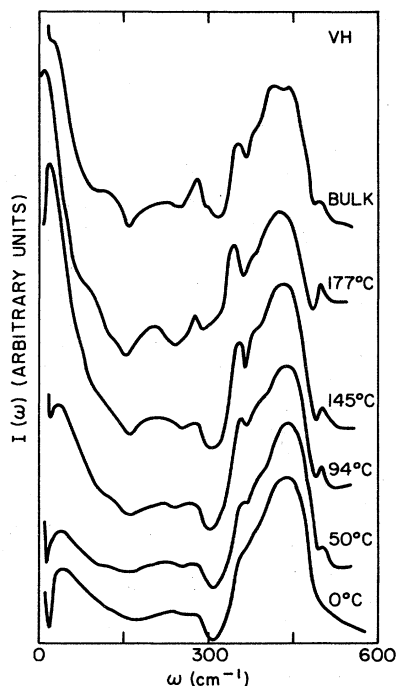


FIG. 5. A comparison of the 80-K VH Raman spectra of rf sputtered a -P films prepared at the indicated T_s . The Raman spectrum of bulk a -red-P is also shown. The VH designation corresponds to incident and scattered fields perpendicular and parallel to the scattering plane, respectively.

density of states of a -P in the higher T_s films.

A comparison of the VH and HH spectra of Figs. 3 and 5 indicates that the features at ~ 280 , 350, 380, and 500 cm^{-1} are rather polarized. Although still measurable, the changes observed in the form of the VH spectra are correspondingly smaller than those in the HH spectra. The totally polarized Raman spectra ($\text{HH} - \frac{4}{3} \text{VH}$) of selected rf sputtered films are shown in Fig. 6. In all of the totally polarized spectra, peaks occur at ~ 350 , 380, and 500 cm^{-1} , except for the 0°C film. The latter indicates a single peak at $\sim 375 \text{ cm}^{-1}$. Several authors^{9,21} have noted that such polarized scattering is enhanced for eigenvectors where local bond lengths are modulated in phase. Beeman and Alben²¹ also suggest that the totally polarized spectrum should peak at lower frequencies than the depolarized VH spectrum for group-V amorphous solids. This suggestion is in qualitative agreement with the spectra presented in Figs. 5 and 6. The occurrence of three distinct, higher optical-band features at ~ 350 , 380, and 500 cm^{-1} in HH, VH, and totally polarized spectra may not, however, be explained by a random coupling of pyramidal units.²² The absence of distinct peaks at 350 and 380 cm^{-1} of the 0°C film could arise due to a broadening of these modes into a single broad peak

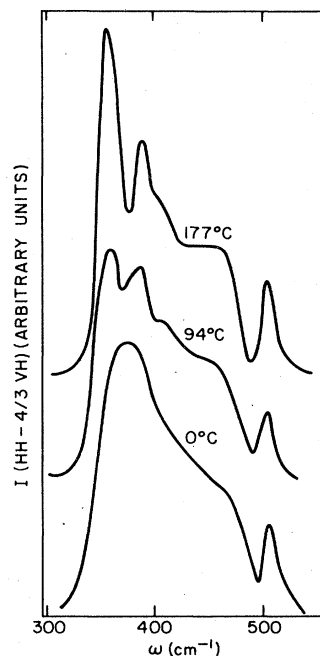


FIG. 6. A comparison of the totally polarized Raman spectra of rf sputtered a -P films prepared at the indicated T_s .

at 375 cm^{-1} . This broadening could result due to additional disorder relative to the higher T_s films. The larger Δk and smaller I_1/I_2 ratio of the 0°C film are consistent with this suggestion.

We have previously shown in Figs. 1, 3, and 5 that marked modifications occur in the Raman and x-ray diffraction spectra as a function of T_s . In Fig. 7 we examine the correspondence between changes in these static and dynamic probes. In Fig. 7(a), the interrelationship of $R_{\text{HH}}(350)$ and I_1/I_2 is shown, while the correspondence between $R_{\text{HH}}(350)$ and $1/\Delta k$ is shown in Fig. 7(b). In both cases, as the HH Raman intensity of the feature at $\sim 350 \text{ cm}^{-1}$ increases, the I_1/I_2 and $1/\Delta k$ values also become larger. As the intensities at 350, 380, and 500 cm^{-1} exhibit similar T_s behaviors, the features at 380 and 500 cm^{-1} are similarly related to the low-angle diffraction parameters. This indicates that the structural correlations, which are probed by the x-ray diffraction measurements, are related to the polarizability correlations examined with Raman scattering. Figure 7(a) indicates an approximate linear variation between $R_{\text{HH}}(350)$ and I_1/I_2 . In contrast, $R_{\text{HH}}(350)$ is a weak function of $1/\Delta k$ at lower values of the latter, while at higher T_s values both $R_{\text{HH}}(350)$ and $1/\Delta k$ increase. These results suggest that the Raman spectra are more directly correlated with variations in the intensity of the low-angle diffraction peak rather than the width of this peak for the sputtering conditions employed here.

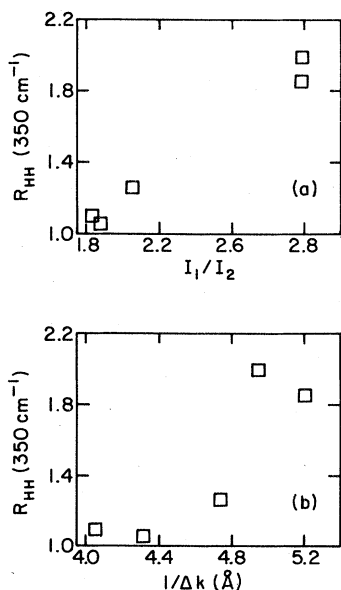


FIG. 7. The interrelationships of the Raman ratio, $R_{\text{HH}}(350 \text{ cm}^{-1})$ and the x-ray-diffraction results for (a) the I_1/I_2 ratio and (b) $1/\Delta k$ values.

DISCUSSION

A recent theoretical Raman study⁹ has emphasized the role of correlated first-neighbor stretching motions in AX_2 glasses in a one parameter, central force model. Such motions lead to a relatively polarized high-frequency band-edge mode in this system and a depolarized VH Raman spectrum that is of the form of the phonon density of states. This study also indicates that if intermediate-range order is present in the amorphous network, then the VH spectra will not resemble the phonon density of states, but may be enhanced for selected modes. While the *a*-P Raman spectra differ from these AX_2 glasses and indicate a more detailed vibrational spectrum, certain qualitative general conclusions of the theory may be applicable.

A comparison of the VH Raman spectra of bulk *a*-P with a neutron scattering experiment²³ indicates differences between the VH spectrum and the density of states that are consistent with the growth of dynamical correlations associated with intermediate-range order. The similarity of the high- T_s films and bulk *a*-P, shown in Fig. 5, imply that intermediate-range order is present in these films. These results indicate the first experimental evidence of intermediate-range order consistent with the theory of Martin and Galeener.⁹ Such order may also, within the general theoretical Raman framework,⁹ modify the polarized Raman component. In contrast to the depolarized spectrum, however, the polarized component is sensitive to both correlations within the first coordination sphere as well as those of longer range.

In Fig. 8 the background subtracted, higher optic band, VH results are shown. The full width at half maximum of these bands, as denoted by the arrows, is observed to increase for the higher T_s films. This is somewhat surprising as the phonon density of states might be expected to become narrower for the more correlated, higher T_s films. In addition, the experimentally determined²³ phonon density of states of bulk *a*-red-P exhibits a narrower bandwidth than the VH Raman spectra of the bulk material or any of the rf sputtered results presented here. This apparent inconsistency is attributed to the presence of intermediate-range order in the bulk material as well as the *a*-P films. An increased coupling to the modes at 350 cm^{-1} of the VH spectra, due to intermediate-range polarizability correlations, could result in an increase in the higher optical bandwidth relative to the phonon density of states.

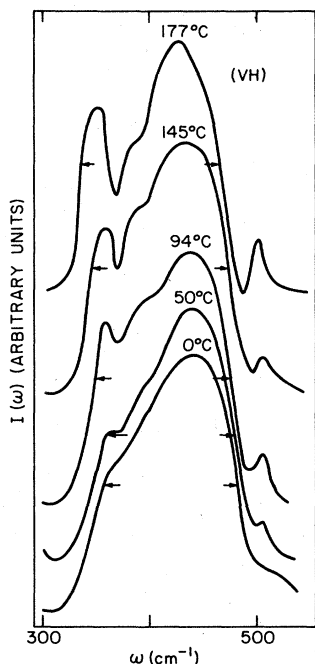


FIG. 8. A comparison of the high-frequency VH Raman spectra of the rf sputtered *a*-P films prepared at the indicated T_s . The arrows indicate the full widths at half maximum of the bands.

Although some modifications in local bond-angle fluctuations may occur and lead to a broadening of the high-frequency VH band at lower T_s values, the growth of selected high-frequency features are attributed to increased intermediate-range polarizability correlations. This is reasonable, since *a*-As films prepared at two temperature extremes indicate similar bond-angle variations, for differences in I_1/I_2 of $\sim 30\%$.²⁴ The increased narrowing of lower frequency peaks and minima in the Raman spectra of Figs. 3 and 5 may also be a consequence on increasing intermediate-range order. This may also apply to the low-frequency Raman peak, below 100 cm^{-1} , which narrows and shifts to lower frequencies with increasing T_s .

The comparison of diffraction and Raman scattering measurements in Fig. 7 indicates that dynamical correlation effects appear to be related to the growth of structural correlations. Similar, less detailed evidence exists in the case of *a*-As.^{4,24} In the limiting case of *a*-Sb, low-angle x-ray-diffraction measurements²⁵ in sputtered films with $T_s \approx 100\text{ K}$ indicate a very weak peak at $k \approx 1.1\text{ \AA}^{-1}$, with $I_1/I_2 \approx 0.1$, while the Raman spectra⁴ are relatively structureless, as is the depolarization

ratio. In order to discuss correlations in more detail it is necessary to consider various structural models for amorphous group-V systems. Most structural models have considered that these systems may be locally viewed as being quasi-two-dimensional in character. An exception to this is the tubular model of Krebs and Gruber¹⁰ which suggests that linear tubular arrays similar to those in Hittorf's P may be present. This model does not, however, yield reasonable agreement with the radial distribution function (rdf) of *a*-P and would require further study of intertubular arrangements to determine if improved agreement with experiment is possible. Other models vary in the extent to which the quasi-two-dimensional systems exhibit interlayer and intralayer structural correlations. The two limiting cases are (a) the random network model for *a*-As of Greaves, Elliot, and Davis,²⁶ which has a relatively random dihedral angle distribution with little interlayerlike correlations, and (b) microcrystallitelike models^{24,27,28} in which parallel, relatively ordered, layers are present. Intermediate to these structures are layer models such as that suggested for *a*-As in which a mixture of staggered and eclipsed dihedral bonding angles are present.²⁴ Additional layer models have been considered for *a*-As by Beeman and Alben²¹ and Popescu.²⁹ All of the above models are assumed to correspond to a given structure of *a*-As, that of presumed lowest energy, given the relaxation procedures employed. These models do not, for example, consider that variations in structure are possible. Such variations are quite graphically indicated by the present *a*-P results as well as those in *a*-As.^{4,5}

While the random network and layerlike models are similar in terms of locally two-dimensional character of the structure they differ in the extent to which the layers are ordered within, as well as between, themselves. Beeman has recently calculated³⁰ $I(k)$ for *a*-P using the *a*-As, Greaves-Davis model relaxed to the 102° average bond angle of *a*-P. His results yield a much smaller low-angle peak than that of bulk *a*-P or any of the sputtered films reported here. As the Greaves-Davis model exhibits little layer parallellicity locally, this suggests that a less random, more layerlike model may be more appropriate to *a*-P. If it is assumed, as is reasonable for the P system, that interlayer interactions are relatively weak, then Raman scattering primarily probes dynamic correlations in polarizability within such individual layerlike regions. The Raman spectra will then depend on intralayerlike correlation functions that are in general a function

of both structure and atomic displacements.⁹ Simple structural and dynamical correlation lengths thus may be difficult to obtain directly from experiment, except in the low-frequency Debye-type regime.^{31,32} In contrast, regular structural features either within or between local layerlike regions are required to obtain a diffraction peak. In layerlike models it is assumed that the low-angle diffraction peak is a consequence of interlayer correlations, where various degrees of disorder or "buckling" within the layers are assumed. In this type of model the width of the low-angle diffraction peak is a statistical measure of the average interlayer correlation length. In contrast, the relative intensity of this peak will depend both on intralayer and interlayer correlations. Thus, I_1/I_2 might be interpreted as the fraction of material in which local layers tend, on average, to be parallel.¹⁷ As such, I_1/I_2 would then depend on both intralayer and interlayer correlations.

In bulk *a*-P the I_1/I_2 ratio of 2.3 is significantly larger than the value of ~ 0.4 observed in bulk *a*-As, while the widths of the low-angle peaks are similar. Within a layerlike model this implies a greater degree of intralayer structural correlations in bulk *a*-P. The rdf of bulk *a*-P indicates ~ 8 atoms in the second coordination sphere, while *a*-As has ~ 10 atoms. The larger number of atoms in the second coordination sphere of *a*-As indicates a trend toward increased back-bonding interactions.²⁶ This trend is consistent with increased covalency¹¹ of *a*-P as indicated by a static bond charge³³ in *a*-P that is larger than that of *a*-As by a factor of 1.8. In addition, *a*-P has a narrower bond-angle variation, $\langle \Delta\theta \rangle = 4.3^\circ$ versus 7.1° in *a*-As.^{10,27} The decreased fluctuations in *a*-P from the mean bond angle would result in increasing intralayer order, relative to *a*-As.

An additional indication of increased structural correlations in *a*-P is exhibited by the Raman spectra of bulk *a*-P and *a*-As shown in Fig. 9. The spectra have been scaled by the relation $\omega_{As} = 0.56\omega_P$, so as to yield the maximum correspondence of spectra features in the two systems. The scaling factor of 0.56 agrees with that obtained for the corresponding crystalline, layerlike orthorhombic forms of P and As.³⁴ As Fig. 9 indicates, there is a considerable similarity in the form of the two spectra, suggesting related microscopic structures. The *a*-P data indicate, however, a far greater degree of resolvable features. While this will in part reflect smaller variations in bond angle, it is also a consequence of increased dynamical

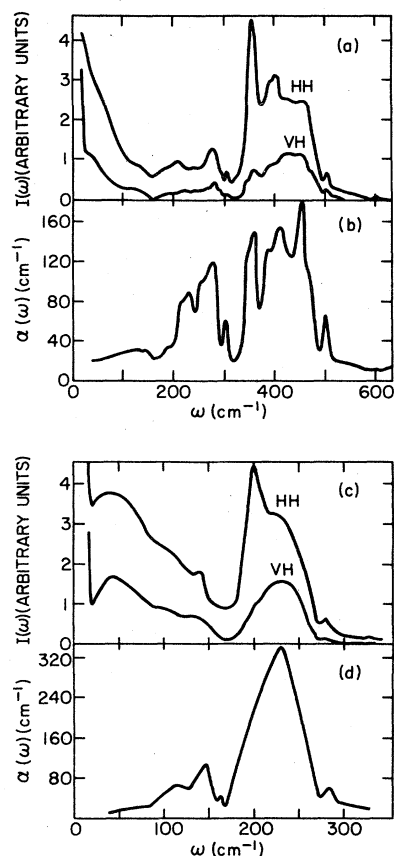


FIG. 9. Comparison of the Raman spectra (a) and infrared absorption coefficients (b) of bulk *a*-red-P with the Raman spectra (c) and absorption coefficient (d) of bulk *a*-As.

correlations that arise from enhanced intralayer structural correlations. This is also consistent with the greater similarity of the VH Raman component and neutron scattering spectra^{4,35} in *a*-As than *a*-P. In *a*-As an increase in metallicity results in increased bond-angle fluctuations and back-bonding interactions, both of which tend to reduce dynamical correlations. In contrast, the greater covalency of *a*-P allows for the potential of a more ordered layerlike structure with reduced interlayer coupling.

CONCLUSIONS

The observed changes in the Raman and x-ray diffraction spectra with T_s , for fixed sputtering conditions, have been suggested to arise from dynamic and static correlations in atomic displacements and positions. The experimental results,

along with recent theoretical work, provide, we believe, the strongest evidence to date for intermediate-range order and related dynamical correlations in amorphous solids. A possible description in terms of a generalized layerlike model in which intralayer- and interlayerlike correlations in structure and interlayer dynamical correlations is suggested. Within this model the growth of intralayerlike correlations with T_g could account for the substantial changes in the high-frequency Raman spectra. In addition, the shift of the low-frequency Raman peak may also be a consequence of increasing the layerlike character of the vibrational modes.³ Modifications of intermediate-range order may, for example, arise from variations in dihedral angle distribution, ring statistics, or more extended network geometrical factors. Further theoretical work is needed to determine if such a layerlike model may account in detail for the diffraction and Raman spectra and their variation. The intense low-angle peak in *a*-P clearly places important constraints on such models. In contrast to most studies in amorphous solids, this work emphasizes the nonuniqueness of the amorphous state and the need for a range of structural models for

a-P. This is also the case for the related *a*-As and *a*-Sb systems where structural and dynamical correlations are also suggested. In contrast to these systems, where weak back-bonding interactions play an increasingly important structural role, *a*-P is more covalent in character. This implies that dominant interlayer van der Waals coupling allows in both the structure and dynamics for a more correlated amorphous solid. As is intuitively reasonable from crystalline solids, structural correlations appear to be a requirement for the high-frequency dynamical correlations. The experimental results in *a*-P further indicate that such correlations appear to be continuously variable.

ACKNOWLEDGMENTS

We wish to thank Dr. Dorn of the firm of Hoechst for the black P sputtering material, R. Messier and J. C. Phillips for stimulating discussions, and D. Beeman for communicating unpublished structural results and for useful discussions. This work was supported by NSF Grant No. DMR7908390.

*Present address: Naval Research Laboratory, Washington, D.C.

¹A. J. Leadbetter and A. J. Apling, in *Proceedings of the 5th International Conference on Amorphous and Liquid Semiconductors, Garmisch-Partenkirchen, 1978*, edited by J. Stuke and W. Brenig (Taylor and Francis, London, 1974), p. 457.

²O. Hemura, Y. Sagara, D. Huno, and T. Satow, *J. Non-Cryst. Solids* **30**, 155 (1978).

³J. C. Phillips, C. A. Beevers, and S. E. B. Gould, *Phys. Rev. B* **21**, 5724 (1980); J. C. Phillips, *J. Non-Cryst. Solids* (in press).

⁴J. S. Lannin, *Phys. Rev. B* **15**, 3863 (1977).

⁵J. S. Lannin, H. F. Eno, and H. L. Luo, *Solid State Commun.* **25**, 81 (1978).

⁶A. J. Leadbetter, P. H. Smith, and P. Seyfert, *Philos. Mag.* **33**, 441 (1976).

⁷R. J. Nemanich and S. A. Solin, *Solid State Commun.* **21**, 273 (1977).

⁸G. Lucovsky and F. L. Galeener, *J. Non-Cryst. Solids* **37**, 53 (1980).

⁹R. M. Martin and F. L. Galeener, *Phys. Rev. B* **23**, 3071 (1981).

¹⁰H. Krebs and H. V. Gruber, *Z. Naturforsch Teil A* **22**, 96 (1967).

¹¹J. S. Lannin and B. V. Shanabrook, *Solid State Commun.* **28**, 497 (1978).

¹²B. V. Shanabrook, J. S. Lannin, and P. C. Taylor, *Solid State Commun.* **32**, 1279 (1979).

¹³S. B. Bailey, R. T. Richard, and E. N. Mitchell, *Rev. Sci. Instrum.* **40**, 1237 (1969).

¹⁴A. J. Stirling and W. D. Westwood, *J. Phys. D* **4**, 246 (1971).

¹⁵R. Messier, Ph.D. thesis, Pennsylvania State University (unpublished).

¹⁶H. R. Klug and L. E. Alexander, *X-ray Diffraction Procedures for Polycrystalline and Amorphous Materials* (Wiley, New York, 1974).

¹⁷S. Bishop and N. Shevchik, *Solid State Commun.* **15**, 629 (1974).

¹⁸L. J. Pilione, R. J. Pomian, and J. S. Lannin, *Solid State Commun.* (in press).

¹⁹R. J. Nemanich, G. Lucovsky, W. Pollard, and J. D. Joannopoulos, *Solid State Commun.* **26**, 137 (1978).

²⁰W. Pollard and J. D. Joannopoulos, *Phys. Rev. B* **21**, 760 (1980).

²¹D. Beeman and R. Alben, *Adv. Phys.* **26**, 339 (1977).

²²G. Lucovsky and J. C. Knights, *Phys. Rev. B* **10**, 4324 (1974).

²³F. Gompf and J. S. Lannin (unpublished).

²⁴H. Krebs and R. Steffen, *Z. Anorg. Allg. Chem.* **327**, 224 (1964).

²⁵B. V. Shanabrook and J. S. Lannin (unpublished).

²⁶G. N. Greaves, S. R. Elliot, and E. A. Davis, *Adv.*

- Phys. 28, 49 (1979).
- ²⁷P. M. Smith, A. J. Leadbetter, and A. J. Apling, *Philos. Mag.* 31, 57 (1975).
- ²⁸R. Bellisent and G. Tourand, *J. Phys.* 37, 1423 (1976).
- ²⁹M. Popescu, Proceedings of the International Conference on Amorphous Semiconductors, Pardubice, 1978 (unpublished).
- ³⁰D. Beeman (unpublished).
- ³¹A. J. Martin and W. Brenig, *Phys. Status Solidi B* 59, 241 (1973).
- ³²R. J. Nemanich [*Phys. Rev. B* 16, 1655 (1977)] has attempted to extract a structural correlation length from Raman spectra using the theory of Ref. 31, extrapolated, however, beyond the Debye-type frequency range.
- ³³J. C. Phillips, *Covalent Bonding in Crystals, Molecules, and Polymers* (University of Chicago, Chicago, 1969).
- ³⁴J. S. Lannin and B. V. Shanabrook, *Proceedings of the 14th International Conference on the Physics of Semiconductors, Edinburgh, 1978*, edited by B. L. H. Wilson (Institute of Physics, Bristol, 1978), p. 643.
- ³⁵A. J. Leadbetter, P. M. Smith, and P. Seyfert, *Philos. Mag.* 23, 441 (1976).